Br. J. exp. Path. (1987) **68**, 53–65

Ultrastructural pathology of iron-loaded rat myocardial cells in culture

Theodore C. Iancu, Hanna Shiloh, Gabriela Link*, Erika R. Bauminger†, Arie Pinson* and Chaim Hershko‡

*Paediatric Research Unit, Carmel Hospital, Faculty of Medicine, Technion-Israel Institute of Technology, Haifa, and the *Departments of Nutrition and Biochemistry and ‡Department of Medicine, Shaare Zedek Medical Center and Hadassah Medical School, and †Racah Institute of Physics, the Hebrew University, Jerusalem, Israel*

Received for publication 11 June 1986
Accepted for publication 28 August 1986

Summary. The pathological changes induced by in-vitro iron-loading or cultured rat myocardial cells were studied. Cells were exposed to ^{59}Fe- labelled ferric ammonium citrate for up to 24 h followed by 24–72 h chase experiment. After 24 h exposure 29% of the total cellular radioactivity was found in ferritin, 10% in non-ferritin heat supernatant and 61% in an insoluble heat-precipitable form. Mössbauer spectroscopy showed a gradual shift from intracellular iron particles less than 1.8 nm in diameter, through particles of intermediate size, to ferritin-like aggregates over 3.0 nm in diameter, reaching about 20% of total iron by 24 h. Ultrastructural studies showed premature damage such as mitochondrial abnormalities and excessive autophagocytosis. Small, 2.0–5.0 nm electron-dense cytosolic particles were noticed at 3 h of iron loading and reached maximal concentrations at 6 h. This was followed by accumulation of the small particles and of typical iron-rich ferritin cores within siderosomes. Because of the limited duration of iron loading and the high concentrations of non-transferrin inorganic iron employed, the present model is more relevant to acute than chronic iron overload. The efficient incorporation of large amounts of iron within ferritin molecules and its subsequent segregation, together with other smaller particles, within membrane-bound bodies, may represent a defence mechanism limiting iron toxicity in the face of advanced cytosiderosis.

Keywords: iron overload, iron toxicity, myocyte cultures, ferritin, haemosiderosis, ultrastructure

Myocardial toxicity is the most significant life-threatening complication of transfusional siderosis in homozygous β-thalassaemia and other iron-loading anaemias requiring continued transfusional therapy (Buja & Roberts 1971). Understanding the pathogenesis of myocardial iron toxicity has been greatly hindered by the inability to reproduce the clinical manifestations of haemochromatosis in experimental animals (Brown *et al.*

Correspondence: Professor Theodore C. Iancu, Paediatric Research Unit, Carmel Hospital, 34362 Haifa, Israel.

1957), probably because of their powerful protective mechanisms against excess iron. In the absence of an in-vivo animal model, attention has been focused in recent years on hepatocyte, Chang cell and myocardial cell cultures for studying the harmful effects of iron (Cox *et al.* 1981; Goto & Listowsky 1983; Jacobs *et al.* 1978; White & Jacobs 1978). Recent studies by Link *et al.* (1983; 1985) have shown that rat myocardial cells in culture are able to assimilate non-transferrin iron at a rate exceeding transferrin iron uptake by 300 to 1; that iron loading results in impaired cellular contractions; that this is associated with increased lipid peroxidation manifested in the accumulation of cellular malondyaldehyde (MDA); and that all of these effects of iron loading are reversible by in-vitro iron mobilization with desferrioxamine.

In view of these correlations, we were interested in examining the ultrastructural alterations associated with in-vitro loading in myocardial cell cultures at conditions identical to those employed in the above studies. These electron-microscopic studies were supplemented by Mössbauer spectroscopy of the same cell cultures in order to quantitate the amount and size of iron particles assimilated by myocardial cells.

Materials and methods

Ham F-10 culture medium (Beth Haemek, Israel) supplemented with $CaCl_2$ $2H_2O$, 135mg/l, penicillin 2×10^5 u/l, streptomycin 0.2mg/l and 10% horse serum and 10% fetal bovine serum (Gibco), was used as growth medium. For iron uptake studies, heterologous serum was replaced by 20% fresh rat serum. For mincing and washing the organs and for trypsinization, Ham F-10 culture medium without Ca^{2+} and Mg^{2+} (H solution) was used. Trypsin (Sigma, grade III) was dissolved in 0.1 w/v% H solution.

Ferritin iron was isolated from tissue homogenates by the method of Fulton & Ramsay (1960). This method is based on the separation of heat-resistant supernatant from heat-precipitable insoluble (haemosiderin) iron, and further separation of ferritin from the heat-stable supernatant by ammonium sulphate precipitation. Total non-haem iron was determined by the method of Torrance and Bothwell (1968).

Cell cultures

Isolated heart cells were obtained from 1 day old rats by a slight modification of previously published methodology (Yagev *et al.* 1984). After trypsinization, the pooled cells were diluted in growth medium to a final density of 9×10^5 to 1×10^6 cells/ml and seeded in 2 ml aliquots into a 35 mm Petri dish (Falcon 3001). This concentration yielded after 24–36 h an almost confluent layer of cells. Experiments were performed at 5 days of culture when over 80% of the cells were beating myocardial cells. Continued viability of cultured iron loaded cells was documented by supravital dye exclusion and by the absence of enzyme (lactic dehydrogenase-LDH) leakage into the culture medium following 24 h iron loading.

Radioiron labelling. $^{59}FeCl_3$ (specific activity 10 to 15 μCi per microgram, Amersham International) was diluted in 0.005 M HCl and mixed with sufficient sterile ferric ammonium citrate (BDH) to provide a concentration of 100 μg/ml elemental iron. 0.2 ml of this solution was added to 0.8 ml cells in culture medium to provide a final iron concentration of 20 μg/ml. At the end of incubation, culture plates were washed twice with 1 ml of cold culture medium. The cells were scraped and transferred into counting tubes by means of a 'rubber policeman' and resuspended in 0.5 ml culture medium. ^{59}Fe activity was determined in an automatic well-type scintillation counter (Auto-Gamma, Model 5360, Packard Instrument Co., Inc. Downers Grove, Ill).

Mössbauer spectroscopy. Cells for Mössbauer studies were prepared at conditions identical to those of all studies except for the use of iron

enriched to 90% ^{57}Fe for the in-vitro loading of cultured cells at a concentration of 20 μg iron/ml. ^{57}Fe was supplied in the form of ferric ammonium citrate. Cells were incubated with ^{57}Fe for 0.5, 1, 3 or 24 h. In addition, chase studies were performed following 24 h incubation by washing the cultures and continued incubation with cold iron for 24 and 72 h. For each measurement, cultures from five culture plates were pooled, transferred into lucite cells and frozen in liquid nitrogen until Mössbauer measurements. A conventional Mössbauer spectrometer together with a 100 mCi ^{57}Co rhodium source were used. The samples were contained in cryostats permitting absorption measurements to be made at any temperature between 1.5 K and 300K. Temperatures below 4.1 K were obtained by pumping on helium.

Ultrastructural studies

Control specimens. In order to distinguish ultrastructural changes induced by the presence of iron within the medium from those occurring spontaneously with time, duplicate aliquots were processed for transmission electron microscopy, as described below. Control specimens, of cells not exposed to iron, were obtained at 0 h (5-day-old cultures) and at 48, 72 and 96 h.

Exposure to inorganic iron. In our earlier study (Link *et al.* 1985) we found that the highest fractional uptake of iron, presented as radioiron-labelled ferric ammonium citrate, is observed at a concentration of 20 μg/ml. Accordingly, in all subsequent studies this concentration of ferric ammonium citrate was used. Five-day-old cultured cells were studied after exposure to iron at 30 min, 1, 3, 6 and 24 h. In addition, specimens were obtained after 24 h exposure to iron followed by 24, 48 and 72 h chase. These cells were therefore comparable to control cells aged 5 days plus 48, 72 and 96h. The chase experiments were performed by washing out the iron-containing medium with fresh, iron-free medium.

Electron microscopy. Cells from control cultures and after exposure to iron were covered by 2.5% cold phosphate-buffered glutaraldehyde for 1 h, post-fixed in 1% osmium tetroxide for 1 h, and dehydrated in graded ethanol solutions. The cultures were detached from the plates by adding 2 ml of propylene oxide and transferred thereafter to propylene oxide-containing tubes for 10 min. The monolayers were infiltrated with an equivolume mixture of Epon and propylene oxide and embedded in Polarbed 812 (Polaron, Watford, UK). Five blocks were prepared from each culture and four grids from each block were cut at 60 nm and mounted on 300 mesh copper grids. Half of the grids from each specimen were left unstained and the remainder were either conventionally stained with uranyl acetate and lead citrate, or only with lead citrate for 2 min. All specimens were viewed and photographed with a Jeol JEM 100 S electron microscope.

Results

Measurements of iron uptake. The cumulative uptake of labelled ferric ammonium citrate at a concentration of 20 μg elemental iron per ml was studied in the presence of 20% rat serum (total iron binding capacity 0.62 μg/ml). There was a rapid initial phase of iron uptake reaching 9% at 3h, followed by a slower rate of iron uptake reaching 16% at 24h. ^{59}Fe counts of the culture medium in chase studies lasting for up to 72h showed no indication of spontaneous iron release from cells. Fractionation of cellular radioactivity after 24 h of incubation at 37°C in serum-supplemented culture medium showed $29 \pm 2\%$ in ferritin, $10 \pm 1\%$ in non-ferritin heat resistant supernant and $61 \pm 2\%$ in an insoluble, heat precipitable form.

Mössbauer studies. All iron detected by Mössbauer spectroscopy was trivalent. Table 1

Table 1. Intracellular distribution of iron aggregates estimated by Mössbauer spectroscopy

Incubation time (h)	Particle size					
	< 1.8 nm		1.8–3.0 nm		> 3.0 nm	
	μg/10^7 cells	per cent	μg/10^7 cells	per cent	μg/10^7 cells	per cent
0.5	0.8	55±5	0·7	45±5	0	0
1	1.3	50±5	0.9	38±5	0.3	12±2
3	2.8	50±5	1.9	34±5	0.8	15±2
24	1.9	25±5	4.3	58±5	1.3	17±2
24+24 chase	2.2	30±5	3.9	52±5	1.4	18±2
24+48 chase	1.6	25±5	3.6	55±5	1.3	20±2

describes the absolute amounts of iron per 10^7 cultured cells as well as the relative proportion (%) of total cellular iron according to particle size: iron aggregates with a diameter greater than 3.0 nm and a spectrum similar to ferritin; iron aggregates between 1.8 and 3.0 nm; and aggregates smaller than 1.8 nm. These were quantified by determining the relative areas of ferritin-like sextet and the doublet on Mössbauer spectra obtained at 4.1 K and 1.5 K respectively.

Significant iron uptake could be demonstrated as early as 30 min after exposure to high iron concentrations, with a gradual levelling-off by 24 h, in line with previous studies employing ^{59}Fe. Following replacement of the culture medium by a low-iron solution, there was only a very slight reduction in total iron content within the next 24 h. There was a gradual shift with time from iron aggregates of the smallest diameter to medium- and large-sized particles. The proportion of aggregates smaller than 1.8 nm dropped from 55% at 30 min to 25% by the end of the study, whereas particles greater than 3.0 nm increased from nil to 20%. Likewise, the absolute amount of < 1.8 nm particles dropped from a maximum of 2.8 μg/10^7 cells at 3 h to 1.6 at 72 h, whereas medium-sized particles increased from 1.9 to 3.6 μg and > 3.0 nm particles from 0.8 to 1.3 μg/10^7 cells within the same time interval. The course of events indicating a gradual growth of the particles, was largely completed by 24 h of iron loading.

Ultrastructural studies

Control (5-day-old) cultures (0 h). Two cell populations were identified within all cultures examined. Beating cells, or myocytes, clearly contrasted with non-beating cells, or fibroblasts (Friedman *et al*, 1980). In the 5-day-old cultures (0 h) there were about 80% beating myocytes and 20% fibroblasts. The following are some morphological characteristics of these cells:

Myocytes. The main feature of muscle-cells was the presence of myofibrils (Fig. 1*a*). Mitochondria were conspicuous, some were large and elongated and contained densely packed cristae. Lysosomes were rare in cells from initial (5 day-old) cultures. The Golgi apparatus, rough endoplasmic reticulum (RER) and endocytic vesicles were easily identified. Smooth endoplasmic reticulum (SER) vesicles were rare, while ribosomes and glycogen β-particles were abundant.

Fibroblasts. These cells did not contain myofibrils. Their RER was distended, mitochondria were smaller and with fewer cristae and practically no lysosomes were seen in cells of early cultures. Glycogen β-particles, ribo-

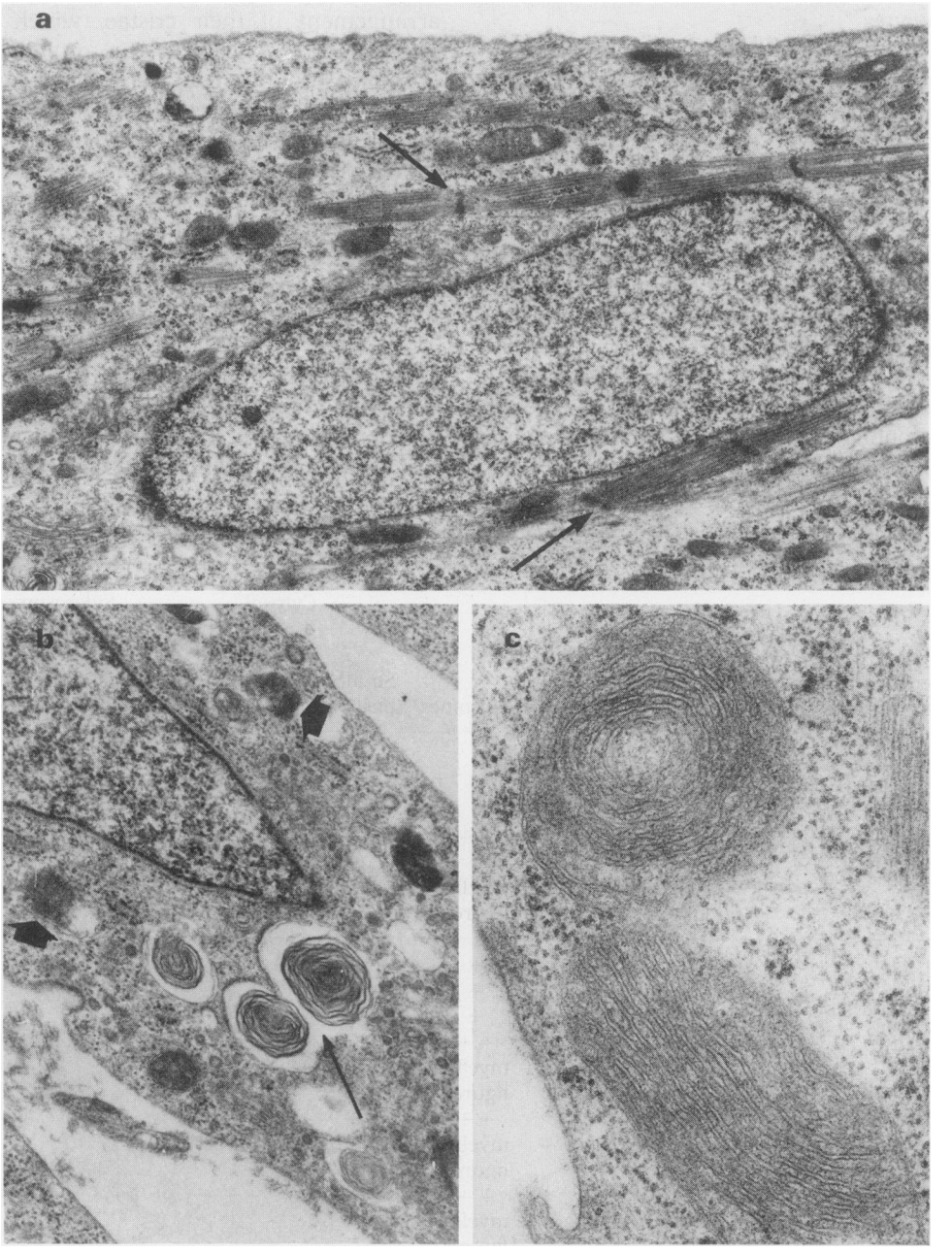

Fig. 1. Electron micrographs of rat heart cells cultured in iron-free medium; *a*, normal appearance of myocyte at 0 h, showing myofibrils with Z bands (arrows); *b*, 4 days from 0 h: myocytes display myelin-like figures (arrow) and bodies with amorphous content (broad arrows); *c*, high magnification of part of a myocyte, 4 days from 0 h, showing curled and concentric mitochondrial cristae. Note absence of matrix granules. Uranyl acetate, lead citrate. *a*, × 12000; *b*, × 20000; *c*, × 40000.

somes and endocytic activity were similar to myocytes.

The changes occurring in cells cultured in iron-free and iron-supplemented medium are summarized in Table 2.

Cells cultured in iron-free medium (controls, 4 days from 0 h)

Myocytes. The main change occurring with time was a progressive increase in the frequency and size of membrane-bound bodies. Some were apparently empty, electron-lucent, while others contained concentric myelin-like membranes or amorphic debris (?autophagosomes) (Fig. 1*b*). Mitochondria displayed pronounced heterogeneity, not only in size and form, but also in the arrangement of their cristae, which frequently were concentric (Fig. 1*c*). Matrix granules, although few, were seen in mitochondria in all stages, except for the last sample at 4 days (9 day old cultures). It should be noted, however, that even in the latest specimens, most cells, including those with autophagosomes, had normal appearing nuclei, normal glycogen content and no other abnormalities except for those described in lysosomes and mitochondria.

Fibroblasts. These cells also showed a progressive increase in membrane-bound bodies, apparently lysosomes. Minor mitochondrial abnormalities were also noticed,

Table 2. Effects of time and exposure to iron on cultured myocytes

Experimental condition and time	Mitochondrial features	Phagosomes*	Cytosol		Siderosomes	
			Small Fe particles	Ferritin iron poor and intermediate	Ferritin iron rich	Haemaosiderin
Iron free Day 2	matrix granules +	+	−	−	−	−
Iron free Day 3	matrix granules +	++	−	−	−	−
Iron free Day 4	vacuolated + no matrix granules	+++ myelin figures	−	−	−	−
Iron 1 h	matrix granules +	+	−	−	−	−
Iron 3 h	matrix granules +	+	+	−	−	−
Iron 6 h	matrix granules +	+	++	+	−	−
Iron 24 h	vacuolated + matrix granules +	++ myelin figures	++	++	+	++
Iron 24 h 24 h chase	vacuolated ++ matrix granules ++	++ myelin figures	+	+++	++	+++
Iron 24 h 48 h chase	matrix granules +	++ myelin figures	+	+++	++	+++
Iron 24 h 72 h chase	wide cristae + no matrix granules	+++ myelin figures	+	+	++	+++

* Without electron-dense particles or aggregates.

−, absent; + to +++, refers to approximate number in micrographs of identical magnification.

mainly in the last specimen, 4 days after the initial observation.

No electron-dense ferritin-like particles were seen either in the cytosol or lysosomes of control cells of both types, at any stage of observation.

Effects of iron exposure on cultured cells

Definition of iron-containing compounds. We identified small electron-dense iron-containing particles, (2.0–4.0 nm in greatest diameter) which were irregular and heterogeneous. They were randomly distributed in the cytosol, rarely in mitochondria and nuclei, or accumulating within membrane-bound bodies (lysosomes–siderosomes) in both myocytes and fibroblasts. Because of their size and form, these particles did not qualify as classical ferritin iron cores (Richter 1978; Iancu 1983; Richter 1984). In contrast, typical 'iron-rich' ferritin particles were regular, homogenous and larger (about 6.5 nm unstained, 7.0–9.0 nm stained). They were seen in clusters, mainly in siderosomes. Similarly to rat liver (Richter 1984), these particles were arranged as groups, arrays or chains without touching each other and with a centre-to-centre distance not smaller than 11.0 ± 0.5 nm. Among the cytosol particles, some were faint in electron-density and small in diameter (approximately 5.5 nm), similar to the population of 'iron-poor' ferritin recognized in other iron loaded cells (Iancu & Neustein 1977; Iancu 1983). Other particles were of medium electron-density and intermediate size (6.0 nm). Haemosiderin-like material was defined ultrastructurally as a heterogeneous compound usually found in siderosomes, containing aggregates of smaller particles and amorphous electron-dense material.

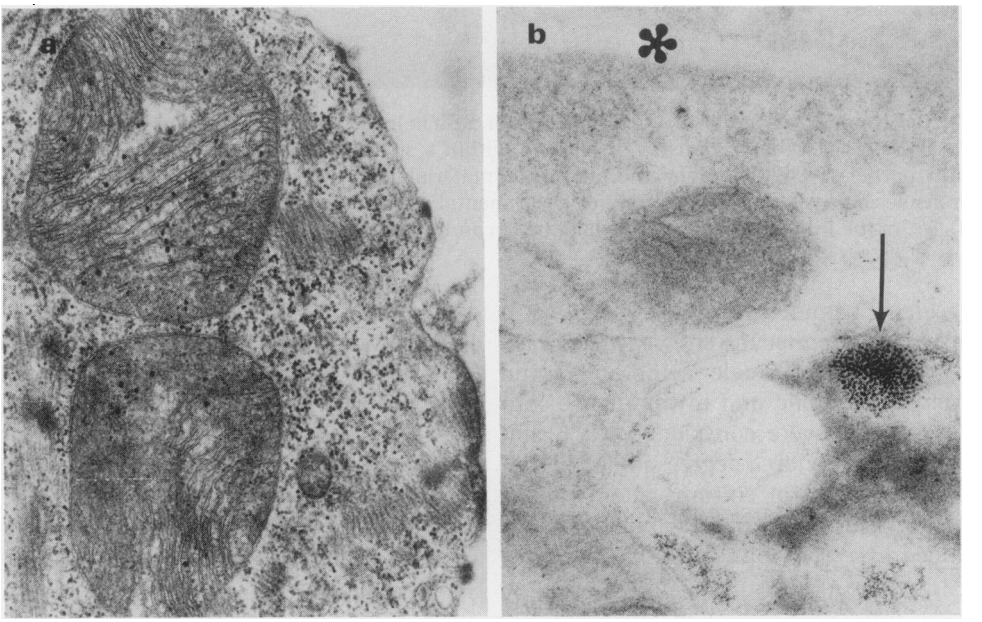

Fig. 2. Electron micrographs of rat heart cells cultured in iron-enriched medium; *a*, myocyte after 3 h exposure to iron. Mitochondria with curled cristae and many matrix granules as well as cytosolic content of normal appearance are seen; *b*, after 24 h iron exposure typical iron rich particles are segregated within a compound lysosome (arrow). Other particles with variable iron content, occasionally coalesced so that individual particles cannot be resolved anymore, are also present in such bodies. *, No particles are seen in the adjacent intercellular space. *a*, lead citrate, × 37500; *b*, unstained, × 70000.

Fig. 3. Electron micrograph of myocyte cultured for 24 h in iron-containing medium and examined after 24 h chase: particles of various size coalesced within a siderosome cannot be resolved as individual ferritin particles. They form haemosiderin-like material (H), similar to the haemosiderin seen in siderosomes during naturally occuring or experimental cytosiderosis. Within the cytosol, many ferritin particles, of the iron-poor and intermediate type, can be identified. Unstained, × 105000.

Myocytes. Examined after 1,3,6 and 24 h iron exposure monocytes showed an increasing frequency of single-membrane-bound bodies. Osmiophilic and myelin-figure-containing bodies were conspicuous at 6 and 24 h respectively, to a degree similar to that observed in control cultures after 3 days. Mitochondrial abnormalities noted at 3 h included excessive mitochondrial heterogeneity and curling of cristae (Fig. 2*a*). The proportion of abnormal mitochondria increased within the first 24 h of iron exposure. Thereafter, the main pathological features were vacuolated mitochondria or mitochondria with wide cristae. These changes, similar to those seen in iron-free cultures in the late samples, appeared much earlier in iron-exposed cells. There was no

Fig. 4. After 24 h iron exposure and 72 h chase; *a*, large amounts of electron-dense aggregates (H, haemosiderin-like material) are seen within an unidentified cell, displacing and replacing cellular content. The adjacent myocyte (M) and fibroblast (F) have a near-normal appearance; *b*, same specimen as in *a*. Higher magnification of a myocyte showing iron accumulation within various membrane-bound bodies. Not differences between small, isolated or coalesced particles (small arrows) and larger typical ferritin particles (broad arrow). S, compound siderosome. *a*, Unstained, × 20000; *b*, × 105000.

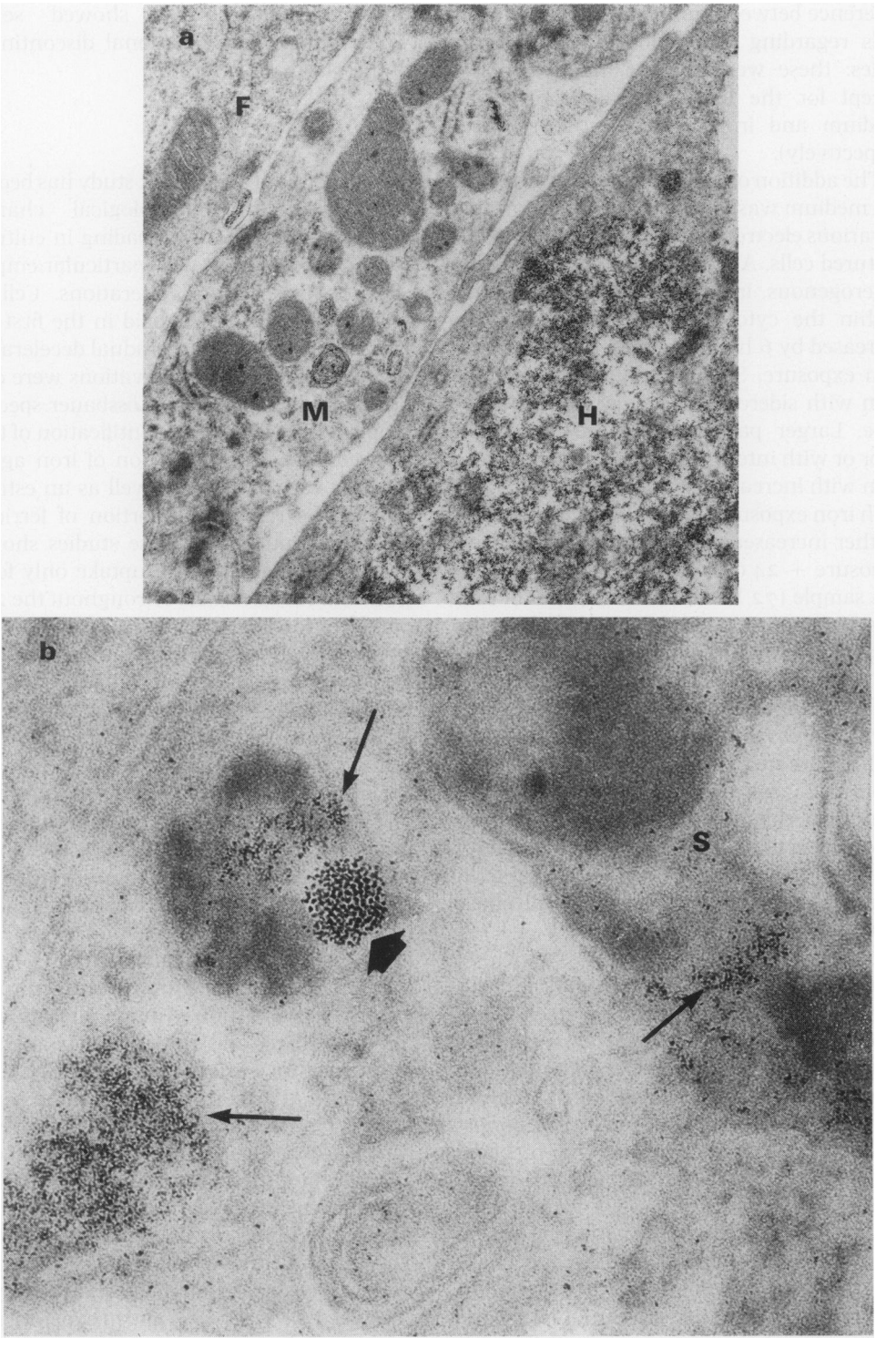
a
F
M
H
b
S

difference between iron-exposed and control cells regarding mitochondrial matrix granules: these were present in all samples, except for the last one (day 4 iron-free medium and iron 24 h + 72 h chase, respectively).

The addition of ferric ammonium citrate to the medium was followed by the appearance of various electron-dense particles within the cultured cells. After 3 h, small (2.0–4.0 nm) heterogenous, irregular particles were seen within the cytosol. This type of particles increased by 6 h and decreased after 24 h of iron exposure. Similar small particles were seen with siderosomes beyond 6 h of exposure. Larger particles (5.5–6.0) nm, iron poor or with intermediate iron content, were seen with increasing frequency after 6 h and 24 h iron exposure (Fig. 2*b*). Their frequency further increased in samples after 24 h iron exposure + 24 or 48 h chase (Fig. 3). In the last sample (72 h chase) the amount of iron was so large as to displace and replace the normal cell content beyond recognition (Fig. 4*a*). At this stage there were only few particles in the cytosol. Typical iron-rich ferritin cores (about 6.5 nm diameter) which had been noted already after 24 h of iron-exposure, were more conspicuous after the chase experiments (Fig. 4 *b*). The accumulation of coalesced particles within siderosomes was similarly noticeable beyond 24 h of exposure and remained so in all chase experiments.

Fibroblasts. Changes in non-muscle cells were less distinct in the various stages of iron exposure and mitochondrial abnormalities more discrete than in myocytes. Similarly to myocytes, small particles were noticed beyond 3 h of exposure and were almost absent from the cytosol after 24 h, being replaced by characteristic ferritin cores, mainly of the iron-poor variety. Typical iron-rich ferritin particles were also seen in the advanced stages of iron loading and chase experiments, but only in siderosis. In general, the longer the exposure to iron, the more siderosomes were noted. Cells with numerous siderosomes showed severe vacuolization and occasional discontinuity of the plasma membrane.

Discussion

The objective of the present study has been to characterise the pathological changes induced by in-vitro iron-loading in cultured rat myocardial cells, with particular emphasis on ultrastructural alterations. Cellular ^{59}Fe uptake was most rapid in the first few hours of loading with a gradual deceleration subsequently. These observations were confirmed and extended by Mössbauer spectroscopy, which provided quantification of total iron content, the proportion of iron aggregates of various sizes, as well as an estimation of the relative proportion of ferric as against ferrous iron. These studies showed that at all phases of iron uptake only ferric iron could be identified. Throughout the 24 h period of loading there was a gradual shift from particles less than 1.8 nm in diameter, through particles of intermediate size, to ferritin-like aggregates over 3.0 nm in diameter, reaching about 20% of the total cellular iron by 24 h.

Our ultrastructural studies were focused on two additional aspects: *a*, morphological organelle changes associated with iron-induced injury and *b*, the manner in which iron is assimilated by the cell and segregated into ferritin, membrane-bound organelles, and other cellular compartments.

When compared with control cultures, iron-loaded cells showed minor alterations in the early stages and more severe changes in the later ones, without necessarily leading to cell death, at least during the limited period of observation. That mitochondrial respiration was preserved following short-term exposure to iron, was supported by the presence in all stages, except the latest, of numerous matrix granules in mitochondria. These granules have been noted to disappear in the early stages of damage, in hepatocytes (Desmet & De Vos 1984) and in experimental anoxia of rat myocytes (Schwartz *et al.*

1984). Notwithstanding the persistance of matrix granules, we concluded that the early appearance (after 3–24 h) of abnormalities in iron-exposed cells, otherwise noted only after 3 to 4 days in non-exposed cells, indicated deleterious effects of iron.

The first ultrastructural evidence of intracellular iron accumulation was the appearance of small heterogeneous cytosolic particles after 3h, with subsequent decrease of their frequency in the cytosol and concomitant segregation within siderosomes. The origin and nature of these small cytosolic particles is at present unclear. Artifactual 'particles' produced by osmium fixation are dissimilar, having a linear form and being usually associated with membranes. The distribution of the small iron particles argues for their genuineness: they were not seen in intercellular spaces, nor within the RER or SER. Their size and form was similar to that of some particles found in siderosomes of rat liver cells and described as divested ferric oxyhydroxide $(FeOOH)_x$ (Richter 1984). Their presence in the cytosol at an early stage, when siderosomes contained little iron, makes ferritin degradation an unlikely source. We assume that they represent inorganic iron aggregates, probably $(FeOOH)_x$ in microcrystalline form, which were unable to enter apoferritin molecules, either because of a limited amount of apoferritin or because of factors such as buffer, oxidant and protein concentrations (Clegg *et al.* 1980). It is possible that some of the haemosiderin-like material, mainly that noted in the early stages of overload, originates in the small iron-containing particles and not in degraded or divested ferritin.

In attempting to correlate these morphologic observations with the Mössbauer measurements described above, one should bear in mind that the electron-density of iron particles smaller than 2.0 nm diameter may be too low for their identification within unstained cells examined by transmission electron-microscopy. Particles with a diameter of about 2.0 nm or larger apparently correspond to the fraction of the larger iron aggregates measured by Mössbauer spectroscopy. This difference in sensitivity of methods used may explain why there has been no electron-microscopic evidence of iron uptake prior to 3 h of incubation, though nearly one third of the total iron uptake has already been completed after 1 h of incubation.

Other electron-dense particles, with morphological characteristics of ferritin of various types, were noted in increasing amounts, first in the cytosol and later in siderosomes. This is in keeping with the cellular reaction to ongoing and long-term iron exposure and the generally accepted pathway of intracellular iron storage (Iancu & Neustein 1977; Iancu 1983; Hernandez–Yago *et al.* 1980; Richter 1978; 1984).

Taken together, all these observations indicate a gradual build up of ferric iron aggregates, with or without the protein shell of apoferritin. The process starts with the formation of the smallest particles, undetectable by electron microscopy, and continues with the appearance of small 2.0–5.0 nm cytosol particles, subsequently seen in siderosomes as well. Typical ferritin molecules noted in the following sequences, are also segregated in siderosomes and haemosiderin-like material is formed in some of these organelles which have features characteristic of chronic iron overload.

Because of the short exposure period and the relatively high concentration of toxic, unbound inorganic iron to which the cells were exposed, the present model may be more analogous to acute than chronic iron overload. It is nevertheless relevant to the study of long-term effects, since no signs of acute damage were noted to the extent which would interfere with the handling of iron by exposed cells. The study demonstrates that heart cells are capable of reacting defensively against excess iron by formation of particles, including typical ferritin, and their segregation in siderosomes, thus avoiding and delaying cell death.

Clinical and experimental observations have shown that iron toxicity to parenchymal cells increases after the reticuloendothe-

lial system (RES) has been saturated by iron (Iancu *et al.* 1977; 1985). As myocardial damage is a late manifestation of iron overload, it is possible that heart toxicity occurs only after both RES and parenchymal saturation (Cox *et al.* 1981). Under such conditions myocytes may react in a manner similar to that found in cultures of newborn rat cells. Thus our experimental model may provide useful information not only on the pathogenesis of iron-induced damage to myocardial cells, but also in evaluating the therapeutic potential of chelating drugs which have already been shown to reverse the functional and biochemical effects of iron loading in these cells (Link *et al.* 1985).

Acknowledgements

This study was supported in part by a grant awarded to T.C.I. by the Milman Fund for Paediatric Research, and by grants no. 2851/82 of the United States-Israel Binational Foundation and no. HL34062-01A1 of the National Heart, Lung and Blood Institute, awarded to C.H., and grants from the Israel Academy of Sciences and Humanities and the Rivka and Salomon Benador Foundation for Heart Research awarded to A.P. The authors are grateful to Yudith Regev for the photographic work and to Dr A. Luder for help with the manuscript.

References

Brown E.B., Dubach R. & Smith C.H. (1957) Studies in iron transportation and metabolism. X. Long term iron overload in dogs. *J. Lab. Clin. Med.* **50**, 862–893.

Buja L.M. & Roberts W.C. (1971) Iron in the heart: etiology and clinical significance. *Am. J. Med.* **51**, 209–221.

Clegg G.A., Fitton J.E., Harrison P.M. & Treffry A. (1980) Ferritin: Molecular structure and iron-storage mechanisms. *Prog. Biophys. Mol. Biol.* **36**, 56–86.

Cox P.G., Harvey N.E., Sciortino C. & Byers B.R. (1981) Electron-microscopic and radioiron studies of iron uptake in newborn rat myocardial cells in vitro. *Am. J. Pathol.* **102**, 151–159.

Desmet V.J. & De Vos R. (1984) Structural analysis of acute liver injury. In *Mechanisms of Hepatocyte Injury and Death.* Eds. D. Keppler, H. Popper, L. Bianchi & W. Reutter. Lancaster: MTP Press Ltd, pp. 11–30.

Friedman I., Schwalb H., Hallag H., Pinson A. & Heller M. (1980) Interactions of cardiac glycosides with cultured cardiac cells. II. Biochemical and electron microscopic studies on the effects of ouabain on muscle and non-muscle cells. *Biochim. Biophys. Acta.* **598**, 272–284.

Fulton J.V. & Ramsay W.N.M. (1960) The distribution of radioactive iron between ferritin and haemosiderin in rat tissues. *Biochem J.* **74**, 24P (Abstr).

Goto Y. & Listowsky I. (1983) Ferritin synthesis and iron incorporation in cells grown in transferrin-free media. In *Structure and Function of Iron Storage and Transport Proteins.* Eds. I. Urushizaki, P. Aisen, I. Listowsky & J.W. Drysdale. Amsterdam: Elsevier, pp.117–120.

Hernandez-Yago J., Knecht E., Martinez-Ramon A. & Grisolia S. (1980) Autophagy of ferritin incorporated into the cytosol of Hela cells by liposomes. *Cell Tissue Res.* **205**, 303–309.

Iancu T.C. & Neustein H.B. (1977) Ferritin in human liver cells of homozygous beta-thalassaemia: Ultrastructural observations. *Br. J. Haematol.* **37**, 527–535.

Iancu T.C., Landing B.H. & Neustein H.B. (1977) Pathogenetic mechanisms in hepatic cirrhosis of thalassemia major—Light and electron microscopic studies. In *Pathology Annual. Vol. 12.* Eds. S.C. Sommers & P.P. Rosen. New-York: Appleton-Century-Crofts, pp. 171–200.

Iancu T.C. (1983) Iron Overload. *Mol. Aspects Med.* **6**, 1–100.

Iancu T.C., Rabinowitz H., Brissot P., Guillouzo A., Deugnier Y. & Bourel M. (1985) Iron overload of the liver in the baboon. An ultrastructural Study. *J. Hepatol.* **1**, 261–275.

Jacobs A., Hoy T., Humphrys J. & Perera P. (1978) Iron overload in Chang cell cultures. Biochemical and morphological studies. *Br. J. exp. Path.* **59**, 489–498.

Link G., Urbach J., Hasin Y., Pinson A. & Hershko C. (1983) Beating rat heart cell cultures: As in vitro model of iron toxicity and chelating therapy. *Blood* **62 (Suppl. 1,9)**, 38*a* (abstract).

Link G., Pinson A. & Hershko C. (1985) Heart cells in culture: a model of myocardial iron overload and chelation. *J. Lab. Clin. Med.* **106**, 147–153.

Richter G.W. (1978) The iron-loaded cell—The cytopathology of iron storage. *Am. J. Path.* **91**, 363–396.

RICHTER G.W. (1984) Studies of iron overload. Rat liver siderosome ferritin. *Lab. Invest.* **50**, 26–35.

SCHWARTZ P., PIPER H.M., SPAHR R. & SPIECKERMANN P.G. (1984) Ultrastructure of cultured adult myocardial cells during anoxia and reoxygenation. *Am. J. Path.* **115**, 349–361.

TORRANCE J.D. & BOTHWELL T.H. (1968) A simple technique for measuring storage iron concentrations from formalinized liver samples. *South African J. Med. Sci.* **33**, 9–11.

WHITE G.P. & JACOBS A. (1978) Iron uptake by Chang cells from transferrin, nitriloacetate and citrate complexes. The effects of iron loading and chelating with desferrioxamine. *Biochim. Biophys. Acta* **543**, 217–225.

YAGEV S., HELLER M. & PINSON A. (1984) Changes in cytoplasmic and lysosomal enzyme activities in cultured heart cells: the relationship to cell differentiation and cell population in culture. *In Vitro* **20**, 893–898.